Passivation Theory and its Application to Automotive Systems

Technical Report of the ISIS Group
at the University of Notre Dame
ISIS-15-001
March 2015

Meng Xia[1], Arash Rahnama[1], Shige Wang[2] and Panos Antsaklis[1]
[1]Department of Electrical Engineering
University of Notre Dame
Notre Dame, IN 46556
[2]General Motors R&D,
Warren, MI 48090

Interdisciplinary Studies in Intelligent Systems

The support of the National Science Foundation under Grant No. CNS-1035655 is gratefully acknowledged.

Passivation Theory and its Application to Automotive Systems

A Draft

M. Xia, A. Rahnama, S. Wang and P. J. Antsaklis *

March 12, 2015

Abstract

In this report, we consider a passivation method that uses an input-output transformation matrix. This matrix generalizes the commonly used methods of series, feedback and parallel (or feedforward) interconnections to passivate a system. Through an appropriate design of this matrix, positive passivity levels can be guaranteed for the system. The passivation parameters can be selected by solving an optimization problem such as minimizing the tracking error. As an application of our passivation method, we consider systems with input-output time delay. In automotive systems, time-delays cannot be avoided due to software implementations of the control algorithms. We show that our passivation method can be used to compensate for the time-delay in the controller and improve the closed-loop system performance. To validate our results, we provide simulation results in CarSim and Simulink.

1 Introduction

1.1 Cyber-physical Systems

Modern technology has undoubtedly penetrated the fabric of daily lives in advanced countries. As technology substitutes manual labor, the need for designing smart systems that help us perform certain daily tasks has increased. Consequently, the interconnection amongst these units becomes important as well. Hence it is important to come up with compositional systems that govern these interconnections such that each unit can perform as expected, and without the fear of any intervention that might disrupt the system. This increased reliance on technological advancement accompanied with new advancements in sensing, communications, control and computation have created an emerging class of complex systems called Cyber-physical Systems.

Cyber-physical Systems (CPS) consist of large number of complex yet closely interconnected and integrated units. Examples of CPS may be found in smart transportation systems, smart medical

*Xia, Rhanama and Antsaklis are with the Department of Electrical Engineering, University of Notre Dame, Notre Dame, IN 46556, USA (e-mail: {mxia, arahnama, antsaklis.1} @nd.edu). Wang is with General Motors R&D, Warren, MI 48090, USA (e-mail: shige.wang@gm.com). The support of the National Science Foundation under the CPS Grant No. CNS-1035655 is gratefully acknowledged.

devices, and smart energy systems [1]. Loosely speaking, such systems consist of two primary units: the physical part, which provides the system with a continuous model of the physical world, using ordinary differential equations, and a communication and computational part, which monitors, coordinates, and controls the physical systems. The computational unit includes the software component of the design and requires strong communication links in order to both receive and transfer the data to the physical world [2]. The control of cyber-physical systems presents huge challenges, so does the concern for maintaining their robustness, reliability and security issues. The concepts of dissipativity and, more specifically, passivity based on energy consumption of a dynamic system provide a powerful tool for meeting the challenges that compositional systems produce. Passive systems do not generate energy, but only store or release the energy, which was provided to them. Under right conditions, passivity can present asymptotic stability for zero state detectable (ZSD) systems [3]. Additionally, both negative feedback and parallel interconnections of passive systems stay passive, which means passivity and stability are preserved for large-scale systems consisting of passive stable units [4]. This renders passive designs a suitable candidate for designing cyber-physical systems.

Our work was built upon the premise that an automobile meets all the criteria for a cyber-physical system. An automobile provides a platform consisting of both physical and computational components, both integrated through communication networks. Due to lack of a clear understanding of the complex and tight interactions that results from the integration of different control components, the design of automotive control applications is a complicated problem. The main issue is that most problems with control applications occur in the final stages of the development cycle and correcting these mistakes at this level is both expensive and involves the modification of the design and requirements. As a result, the current common design approach relies on ad-hoc techniques with the goal of reaching the desire outcome through trial and error, which is not a reliable approach. Passivity has been studied as a possible systematic solution to this problem. This approach is beneficial in regards to improving overall system performance, and potentially can help solve the scalability challenges given the increasing integration of more and more control functionalities in vehicles.

1.2 Adaptive Cruise Control for Automotive Systems

The main function of the Adaptive Cruise Control (ACC) is to maintain the desired velocity set by the driver. The ACC needs to adjust its speed based on the desired speed of the vehicle, the speed of the lead vehicle, and the distance between the two cars (the safety component of the design). This means that our system will have a hybrid structure of two modes, one to control vehicle when it is accelerating, and one for when it is decelerating. Passivity has been studied extensively in the field of control design and analysis as a suitable alternative to other nonlinear control techniques [5, 6]. And passivity conditions for hybrid and switched systems are discussed in [6, 7].

The design of the adaptive cruise control (ACC) has been extensively studied, and there are numerous design techniques for deriving the corresponding control laws. Multiple-surface sliding control containing a sliding control, and a switching rule between brake or throttle control was used in [8, 9] which results in a smooth alternation between both controllers by solely relying on the vehicle state and avoiding high frequency oscillation and risk of competing control inputs. This ideal is reached by isolating the upper controller from the switching rule. Optimal control was

used in [10, 11] to design an ACC, and the performance was compared with that of the human driver models. The results are that the performance is much smoother with a faster and better transient response. However, lack of well-defined safety features and due to time delay of the switching rule, specifically for situations involving front cut-in vehicles, lead in collisions in some of the experiments under this design.[12] compares Fuzzy logic and H-infinity approaches for ACC. Overall the performances are slow in these designs, and Fuzzy logic design spends a considerable time performing under the desired velocity. Neural networks, and proportional derivative (PD) type control laws were used in [13, 14].

Model based control for an implementation of an intelligent cruise control was examined in [15]. This design performs well and the vehicle speeds match well in performed experiments. Raza and Ioannou in [16] presented a high-level supervisory control design for vehicle longitudinal control. This supervisory controller processes the inputs from the driver, the infrastructure, other vehicles, and the onboard sensors and sends the appropriate commands to the brake and throttle control. [17] uses optimal dynamic back-stepping control to derive the desired acceleration on the supervisory level. However, most supervisory controllers are based on mathematical models rather than real human behavior. Closer to our work, human behavior is modeled through fuzzy controllers or neuro-controllers for spacing adjustments [18, 19]. Very similar to the idea of passivity, Druzhinina et al. [20] have designed an adaptive cruise control using a Lyapunov function approach. Passivity-based control to hybrid systems under the assumptions that the energy in each mode of the system must be bounded and that the composite energy of all modes (active or inactive) must also stay bounded [21].

1.3 Systems with Input-output Delay

A time delay is defined as the time difference between the moment a control signal is applied and an observable change in the measured output that is the result of the applied signal [22]. Examples of time delays in dynamical systems are computational delays, input delays, and measurement delays. In addition higher order systems can be modeled by low order systems plus a time delay. Delays may introduce poor performance or instability to the closed loop system. In 1950s, Otto Smith introduced a unique predictive control method called the Smith Predictor that compensates for delay outputs using input values stored over a certain time window, and estimating the plant output accordingly [23]. Later this method combined with finite time integrals of the delayed input values was expanded to include unstable plants as well. Accordingly, other control methods for handling time-delayed systems were developed [24]. Adaptive control may be used to control time-delayed systems as well [25, 26]. In adaptive control, the structure of the controller is selected deductively, usually PD or PID. Ortega and Lozano introduced a control version of delay systems, which is capable of handling the uncertainty and accumulated error that is usually the result of predictive control methodologies for time-delayed systems [27]. Many examples of systems including time delays in chemical, biological, mechanical, and electrical systems are given in [28, 29]. A more detailed survey of time delay systems can be found in [30, 31].

The driver control's influence, and the vehicle and driver closed-loop systems have been investigated by many authors [32, 33, 34]. In a vehicle and driver closed-loop system, the motion of the vehicle is usually described by a set of first-order differential equations where the response of the driver combined with a time-delayed human reaction appears as a break-throttle or steering

input term. The driver's action is analyzed by observing the vehicle's deviations with respect to the desired states [32, 34, 35]. The effects of delay due to driver's reaction has been analyzed for car-following models [36, 37]. A small sum of delays that is less than 0.2 seconds does not play an essential role in the optimal velocity control according to [38]. However, for large delays, and since the acceleration of the vehicle depends on its velocity and distance from the preceding and front vehicles, this large delay between the control decision and its exertion becomes problematic. This motivates a large field of research work, some mentioned in [39, 40, 41] and including our work presented in this report that try to address and offer solutions for the problem.

1.4 Summary of Contributions

This report is motivated from the time-delay in automotive systems. As we discussed earlier, the time delay may be due to signal processing delay, sensor measurement delay, or may be due to interactions between different control algorithms implemented in the vehicle. Since the control algorithm is often designed by assuming that the time delay is zero, the presence of time delay may cause system instability and performance degradation. Thus, a method that can compensate for the time delay is desirable. On the other hand, passivity and passivity-based control has shown great promise in the control design of automotive systems. This is due to many properties that passivity can provide, such as stability, compositionality and robustness.

In the present report, our objective is to guarantee passivity of controllers with time delay. Since the passivation parameters can be used to tune the passivity indices of the controller after passivation, the passivated controller can be used to stabilize or passivate another plant. Further, we consider the passivation method that also optimizes system performance, such as minimizing the tracking error. Beyond guaranteeing passivity, desired system performance can also be achieved. In order to solve the optimization problem, we consider a co-simulation framework and non-derivative optimization method such that detailed modeling of the plant is not needed. Moreover, our passivation method can be accommodated in order to consider other performance criteria, such as being a low pass filter by using transfer functions in the passivation method. Finally, simulation results in CarSim and Simulink are provided to validate our theory, where a random time delay was considered and a variety of reference inputs were tested.

It is worth mentioning that passivity itself can be viewed as a system performance criterion since it can guarantee not only stability but also robustness with respect to modeling uncertainties [42, 43]. Under certain conditions, an optimal linear-quadratic-Gaussian (LQG) controller is strictly positive real, thus the controller itself is guaranteed to be stable [44]. Design of strictly positive real controllers using numerical optimization is considered in [45], where the objective function is given by minimizing the closed-loop $\mathcal{H}_2$ norm. Optimality and passivity for nonlinear systems have been studied in [46, 47], where optimality and passivity (with respect to a certain output) are shown to be equivalent. The passivity indices have been used to find optimal model predictive controllers in [48], where the model of the system can be inaccurate. In the present report, by tuning the passivation parameters, system performance such as minimizing the tracking error can be achieved. Although mathematical relations between the performance and the passivity indices were not given, our setup in the co-simulation framework using non-derivative optimization method provide an 'indirect' manner to study the relation between performance and passivity.

The rest of the report is organized as follows. In Section 2, we provide a brief review of

passivity and dissipativity theory. The passivation method using constant parameters and transfer functions is presented in Section 3. The optimization problem to find the passivation parameters is formulated in 4. Simulation results to illustrate the effectiveness of the passivation method through CarSim/Simulink are presented in Section 5. Section 6 concludes the report.

Notation: The signal space under consideration is either the standard $\mathcal{L}_2$ space or the extended $\mathcal{L}_2$ space. The exact space will be clear from the context. We use $\mathbf{H} : \mathbf{u} \to \mathbf{y}$ (or simply H) to denote a dynamical system with input u and output y. We use the notations $u(t)$ and u for a signal interchangeably. We use $G(s)$ to denote the transfer function for a SISO linear system. The n-dimensional identity matrix is denoted by $I_{n\times n}$ or simply I by omitting the dimensions if clear from the context.

2 Background on Passivity Theory

Consider a dynamical system given by an operator $\mathbf{H} : \mathbf{u} \to \mathbf{y}$, where $\mathbf{u} \in \mathcal{U}$ denotes the input and $\mathbf{y} \in \mathcal{Y}$ denotes the corresponding output, and a real-valued function $w(u, y)$ defined on $\mathcal{U} \times \mathcal{Y}$, called *supply rate* [49]. We assume that $\int_{t_0}^{t_1} |w(u, y)|\mathrm{d}t < \infty$, for any t_0, t_1 and any input $u \in \mathcal{U}$.

Definition 1. *An operator* $\mathbf{H} : \mathbf{u} \to \mathbf{y}$ *is said to be* dissipative *with respect to supply rate* $w(u, y)$*, if*

$$\int_{t_0}^{t_1} w(u, y)dt \geq 0, \tag{1}$$

for all $t_1 \geq t_0$*, and all* $u \in \mathcal{U}$*.* □

In particular, we can define passivity and $\mathcal{L}_2$ stability when the supply rate is in particular forms.

Definition 2. *Suppose the system* $\mathbf{H} : \mathbf{u} \to \mathbf{y}$ *is dissipative. It is said to be*

- passive *if* $w(u, y) = u^T y$*;*
- input feedforward passive *(IFP) if there exists a constant* ν *so that* $w(u, y) = u^T y - \nu u^T u$*; we call such a* ν *an IFP level, denoted as IFP*(ν)*;*
- output feedback passive *(OFP) if there exists a constant* ρ *so that* $w(u, y) = u^T y - \rho y^T y$*; we call such a* ρ *an OFP level, denoted as OFP*(ρ)*;*
- input-feedforward-output-feedback passive *(IF-OFP) if there exist constants* δ *and* ϵ *so that* $w(u, y) = u^T y - \delta y^T y - \epsilon u^T u$*; we call such* δ *and* ϵ *passivity levels, denoted as IF-OFP*(ϵ, δ)*;*
- finite-gain $\mathcal{L}_2$ stable *if there exists a constant* $\gamma \neq 0$ *so that* $w(u, y) = \gamma^2 u^T u - y^T y$*, denoted as FGS*$(\gamma)$*.*

Further, if $\nu > 0$*, then the system is said to be* input strictly passive *(ISP); if* $\rho > 0$*, then the system is said to be* output strictly passive *(OSP). Similarly, if* $\delta > 0$ *and* $\epsilon > 0$*, then the system is said to be* very strictly passive *(VSP). The largest IFP level* ν *is called the* IFP index *and the largest OFP level* ρ *is called the* OFP index*, respectively.* □

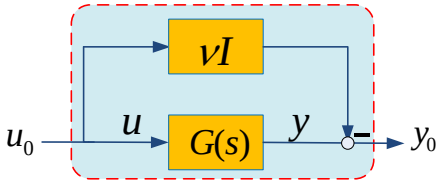

Figure 1: Input feedforward passivity.

Remark 1. *If either one of two passivity indices is positive, we say that the system has an 'excess of passivity'; similarly, if either one of the two passivity indices is negative, we say that the system has a 'shortage of passivity'. Discussion on the difference between passivity levels and passivity indices can be found in [43].*

In Definition 1 and 2, system $\mathbf{H} : \mathbf{u} \rightarrow \mathbf{y}$ can be either linear or nonlinear. If H is linear, then the IFP index can be defined in the following manner.

Definition 3. *The IFP index for a* stable[1] *linear system $G(s)$ is defined as*

$$\nu(G(s)) \triangleq \frac{1}{2} \min_{w \in \mathbb{R}} \underline{\lambda}(G(jw) + G^*(jw)), \tag{2}$$

where $\underline{\lambda}$ denotes the minimum eigenvalue and G^* denotes the conjugate transpose of G. □

In Definition 3, the transfer function $G(s)$ may be rational or irrational. If $\nu \geq 0$, then the system $G(s)$ is called *passive* or *positive real*. If $\nu < 0$, then the system $G(s)$ is not passive and ν can be interpreted as the minimum feedforward gain required for a stable non-passive linear system to become passive [51, 52], as shown in Fig. 1. When $G(s)$ is a single-input-single-output (SISO) system, we can test the passivity of $G(s)$ using its Nyquist plot. If the Nyquist plot of $G(s)$ is in the closed right-hand half of the complex plane, then the system is passive; otherwise, the system is not passive. For the special case when $G(s)$ is rational, if it is passive, then it must satisfy all of the following conditions [51, 53]: (i) stable; (ii) minimum phase; (iii) relative degree 0 or 1.

Remark 2. *For a stable linear system $\mathbf{G} : \mathbf{u} \rightarrow \mathbf{y}$, the IFP index is given by the largest IFP level so that for any $T \geq 0$ and any $u \in \mathcal{U}$,*

$$\int_0^T u^T y - \nu u^T u \, \mathrm{d}t \geq 0. \tag{3}$$

Further, if G has IFP($\tilde{\nu}$), then $\tilde{\nu} \leq \nu$. We show that the IFP index defined in Definition 3 is exactly the largest IFP level of G (see an internal report [54] for proof). Therefore, the two definitions of IFP index of stable linear system are equivalent to each other. □

Consider the feedback configuration as shown in Fig. 2, the passivity and stability of a complex system Σ can be guaranteed from those of systems H and G which are much easier to analyze in practice.

[1] A function $G(s)$ is called *stable* if it is analytic in the closed right half plane of the complex plane, see e.g. [50].

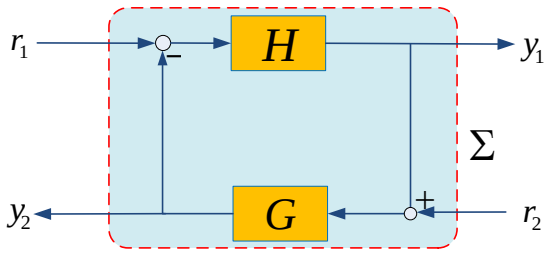

Figure 2: Negative feedback interconnection of system H and system G.

Theorem 1 ([53]). *Consider the feedback interconnection of two systems H and G in Fig. 2.*

1. *If system H and G are passive, then system Σ is passive.*
2. *If system H and G are output strictly passive (OSP), then system Σ is OSP;*
3. *If system H is IF-OFP(ϵ_1, δ_1) and system G is IF-OFP(ϵ_2, δ_2), where $\epsilon_1 + \delta_2 > 0,\ \epsilon_2 + \delta_1 > 0$, then system Σ is finite gain stable (FGS).* □

In Theorem 1, the passivity of both systems G and H is required to guarantee that system Σ is passive. However, it is not necessary for both system G and H to be passive to guarantee the stability of system Σ. For instance, if $\epsilon_1 < 0$ and $\delta_1 < 0$ (i.e. system H is not passive), we require that the system G has passivity levels $\epsilon_2 > -\delta_1 > 0$ and $\delta_2 > -\epsilon_1 > 0$ to compensate for the shortage of passivity of the system H.

Remark 3. *In Fig. 2, we can view system H as a controller and system G as a plant. It can be seen that system Σ is passive only if both the plant and the controller are passive, which may be difficult to achieve in practice.*

If $r_2 = 0$, the feedback system is given by the mapping $\mathbf{r_1} \to \mathbf{y_1}$. We have the following less conservative result.

Theorem 2 ([55]). *Consider the feedback interconnection of two systems H and G in Fig. 2. Assume that $r_2 = 0$.*

1. *If system H has OFP(ρ) and system G has IFP(ν) where $\rho + \nu > 0$, then the system $\mathbf{r_1} \to \mathbf{y_1}$ has OFP$(\rho + \nu)$. Further, the system $\mathbf{r_1} \to \mathbf{y_1}$ is finite-gain stable (FGS) with gain $\gamma \leq \frac{1}{\rho+\nu}$.*
2. *If system H has IFP$(\nu > 0)$ and system G has OFP(ρ) where $\nu + \rho > 0$, then the system $\mathbf{r_1} \to \mathbf{y_1}$ has IFP$(\min\{\nu, \rho + \nu\})$.*

In Theorem 2, the system $\mathbf{u_1} \to \mathbf{y_1}$ is guaranteed to be OSP or ISP (stronger than just being passive). If system H has OFP $\rho < 0$, then the shortage of OFP in system H can be compensated by an excess of IFP of system G with $\nu > -\rho > 0$ so that the feedback system $\mathbf{r_1} \to \mathbf{y_1}$ is guaranteed to be OSP and FGS. Similarly, if system G has OFP $\rho < 0$, then the shortage of OFP in system G can be compensated by an excess of IFP of system H with $\nu > -\rho > 0$ so that the feedback system $\mathbf{r_1} \to \mathbf{y_1}$ is guaranteed to be ISP.

3 Passivation Results

3.1 Passivation Using Constant Parameters

Many methods are known for passivation of non-passive systems, such as series, feedback, parallel or a combination of such schemes [51, 56, 57, 58]. These passivation mechanisms require the system to satisfy certain properties, such as constraints on the relative degree, stability or minimum-phase property of the system. For instance, feedback passivation can only be applied to systems that are of minimum phase and have relative degree less than or equal to one [51]. For systems of the form $G_0(s)e^{-\tau s}$, by using Pade approximations, we know that such systems are approximately non-minimum phase and thus they cannot be passivated through feedback alone.

We consider a passivation method as shown in Fig. 3 (see also [59, 60]), where G is the controller and $m_f, m_s, m_p \in \mathbb{R}$ are called the *passivation parameters*. We assume $m_s \neq m_p m_f$ such that the following matrix M is non-singular, where

$$\begin{bmatrix} u_0 \\ y_0 \end{bmatrix} = M \begin{bmatrix} u \\ y \end{bmatrix} \quad \text{and} \quad M \triangleq \begin{bmatrix} 1 & m_f \\ m_p & m_s \end{bmatrix}.$$

This passivation method includes as special cases the commonly used passivation methods that use

(1) series (by setting $m_p = 0$ and $m_f = 0$);

(2) feedback (by setting $m_p = 0$ and $m_s = 1$); and

(3) parallel interconnections (by setting $m_s = 1$ and $m_f = 0$).

By appropriate choices of the passivation parameters m_f, m_s, m_p, we can obtain the desired passivity levels (ρ_0, ν_0) of the system $\Sigma_0 : \mathbf{u}_0 \to \mathbf{y}_0$. After a few steps of algebraic calculations, it can be seen that the transfer function for Σ_0 is given by

$$\Sigma_0 = \frac{m_p + m_s G}{1 + m_f G}. \tag{4}$$

The following result is immediate.

Lemma 1. *Let a non-passive controller be given by transfer function G and consider the passivation method as shown in Fig. 3. The system $\mathbf{u}_0 \to \mathbf{y}_0$ has passivity levels (ρ_0, ν_0) if and only if the passivation parameters m_f, m_s, m_p are chosen such that Σ_0 given by (4) has passivity levels (ρ_0, ν_0).* □

In general, both sufficient and necessary conditions on m_f, m_s, m_p in order to guarantee passivity of (4) as in Lemma 1 are difficult to obtain. To see this, we can use an LMI formulation [61]. We assume that system Σ_0 has a state-space representation (A_0, B_0, C_0, D_0), where (A_0, B_0, C_0, D_0) are functions of the passivation parameters m_f, m_s, m_p. Note that for systems of the form $G_0(s)e^{-\tau s}$, where G_0 is rational and $\tau > 0$, we can use Pade approximations. To test whether Σ_0 is passive, we can test if the following inequality has a positive definite solution P, where

$$\begin{bmatrix} A_0^T P + P A_0 & P B_0 - C_0^T \\ B_0^T P - C_0 & -(D_0^T + D_0) \end{bmatrix} \leq 0. \tag{5}$$

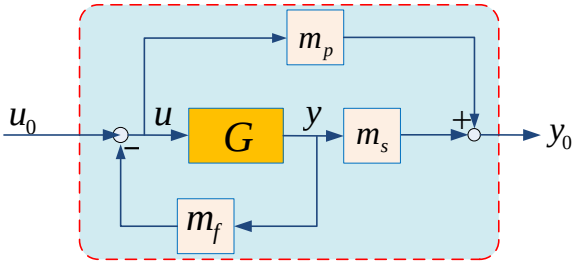

Figure 3: Passivation through series, parallel and feedback interconnections, where $m_p, m_f, m_s \in \mathbb{R}$.

However, the above inequality is generally not linear in the variable P and passivation parameters m_f, m_s, m_p.

The following result provides sufficient conditions on the passivation parameters (i.e. m_f, m_s, m_p) such that the passivity levels of the system Σ_0 can be guaranteed.

Theorem 3. *Consider a controller G which is finite gain stable with gain γ and the passivation method as shown in Fig. 3. Then the system $\Sigma_0 : \mathbf{u}_0 \to \mathbf{y}_0$ is*

1. *OSP with OFP level $\rho_0 = \frac{1}{2}\left(\frac{1}{m_p} + \frac{m_f}{m_s}\right) > 0$, if M is chosen such that*

$$m_p > m_s\gamma > 0, \quad m_s > m_f m_p > 0. \tag{6}$$

2. *ISP with IFP level $\nu_0 = \frac{1}{2}(m_p + \frac{m_s}{m_f}) > 0$, if M is chosen such that*

$$1 > m_f\gamma > 0, \quad m_f m_p > m_s > 0. \tag{7}$$

Proof. See Appendix. □

First, we consider the conditions in (7) for guaranteeing ISP of system Σ_0. $1 > m_f\gamma$ can guarantee the closed-loop of system G and feedback gain m_f to be finite-gain stable according to the small gain theorem. $m_f m_p > m_s$ can be used to adjust the passivity levels ν_0. Next, we consider the conditions in (6) for guaranteeing OSP of system Σ_0. From the condition $m_s > m_f m_p$, we can obtain $m_s\gamma > m_f m_p\gamma$. Then from the condition $m_p > m_s\gamma$, we can obtain $m_p > m_f m_p\gamma$. Further, we have $m_f\gamma < 1$ since $m_p > 0$. Thus, we can also guarantee that the closed-loop of system G and feedback gain m_f to be finite-gain stable from the conditions in (6). Note that the constants m_p and m_s cannot change the stability of the system Σ_0, thereby the system Σ_0 is guaranteed to be finite-gain stable from the above theorem.

Remark 4.

1. *In Theorem 3, the controller G can be either linear or nonlinear provided that G is finite gain stable. In particular, the controller G can be a controller with time-delay.*
2. *The results for guaranteeing passivity (instead of guaranteeing positive passivity indices) of system Σ_0 and a technical proof were presented in [59].*
3. *The above results provide sufficient only conditions for guaranteeing passivity of system Σ_0. The results may be relaxed under certain conditions. In particular, we consider $G = Ke^{-\tau s}$, i.e. when the controller is a PID controller cascaded with time delay.*

Theorem 4. *Consider the controller $G = Ke^{-\tau s}$ where $K > 0$ as shown in Fig. 3. The system $u_0 \to y_0$ is passive if $K|m_f| < 1$ and*

$$m_p + m_s m_f K^2 - |m_p m_f + m_s| K \geq 0. \tag{8}$$

Further, if (8) holds with strict inequality, then system $u_0 \to y_0$ is input strictly passive with input feedforward passivity level ν such that

$$\nu \geq \frac{m_p + m_s m_f K^2 - |m_p m_f + m_s| K}{(1 + |m_f| K)^2}. \tag{9}$$

Remark 5. *Note that in Theorem 4, the parameters m_f and m_s can be either positive, zero or negative. However, in Theorem 3, both parameters are assumed to be positive.*

Proof. The frequency response for system G is given by

$$G(jw) = K(\cos(\tau w) + j \sin(\tau w)).$$

For notational convenience, we define

$$A \triangleq K \cos(\tau w), \quad B \triangleq K \sin(\tau w).$$

such that $G(jw) = A + jB$. The frequency response for system Σ_0 is given by $\Sigma_0 = \tilde{A} + j\tilde{B}$, where

$$\tilde{A} = \frac{m_p + (m_p m_f + m_s) A + m_s m_f K^2}{(1 + m_f A)^2 + (m_f B)^2}, \quad \tilde{B} = \frac{(m_s - m_f m_p) B}{(1 + m_f A)^2 + (m_f B)^2}. \tag{10}$$

Thus, the frequency-dependent IFP for system Σ_0, $\nu_F(\Sigma_0) = \tilde{A}$ can be written into

$$\begin{aligned} \nu_F(\Sigma_0) &= \frac{m_p + (m_p m_f + m_s) K \cos(\tau w) + m_s m_f K^2}{1 + m_f^2 K^2 + 2 m_f K \cos(\tau w)} \\ &\geq \frac{m_p + m_s m_f K^2 - |m_p m_f + m_s| K}{(1 + |m_f| K)^2}, \end{aligned} \tag{11}$$

where the inequality holds for all $w \in \mathbb{R}$. Therefore, the IFP of system Σ_0 satisfies

$$\nu(\Sigma_0) = \min_{w \in \mathbb{R}} \nu_F(\Sigma_0) \geq \frac{m_p + m_s m_f K^2 - |m_p m_f + m_s| K}{(1 + |m_f| K)^2}.$$

If $K|m_f| < 1$, then the system Σ_0 is finite-gain stable based on the small-gain theorem [53, pp. 217-221]. According to condition (8), we have $\nu(\Sigma_0) \geq 0$ and thus system Σ_0 is passive. Further, if (8) holds with strict inequality, then system Σ_0 is input strictly passive with an input feedforward passivity level ν that satisfies (9). This completes the proof. □

Remark 6. *Consider the following two cases to evaluate (11), from which we can obtain upper bounds for IFP levels of Σ_0.*

(1) If $\cos(\tau w) = -1$, *e.g. at frequency* $w = \frac{\pi}{\tau}$, *then we have*

$$\nu_F(\Sigma_0, \frac{\pi}{w}) = \frac{m_p - m_s K}{1 - m_f K}.$$

Thus, the IFP for system Σ_0 *satisfies* $\nu \leq \frac{m_p - m_s K}{1 - m_f K}$.

(2) If $\cos(\tau w) = 1$, *e.g. at frequency* $w = \frac{\pi}{2\tau}$, *then we have*

$$\nu_F(\Sigma_0, \frac{\pi}{2w}) = \frac{m_p + m_s K}{1 + m_f K}.$$

Thus, the IFP for system Σ_0 *satisfies* $\nu \leq \frac{m_p + m_s K}{1 + m_f K}$.

The following result can be seen as a generalization of Theorem 2 for feedback interconnections. In Theorem 2, the plant and the controller have to satisfy certain constraints, e.g. one of them has to be more than passive if the other one is less than passive. If such constraints cannot be satisfied, then we can design the passivation parameters so that the passivity of the feedback system can still be guaranteed. The following result is immediate from Theorems 2 and 3.

Theorem 5. *Consider the feedback configuration in Fig. 6, where* r_1 *can be seen as the reference to the controller* G. *Assume that plant* H *has OFP level* $\rho < 0$. *If the passivation parameters are chosen such that*

$$\nu_0 = \frac{1}{2}(m_p + \frac{m_s}{m_f}) > -\rho,$$

and (7) is satisfied, then the system $\Sigma : \mathbf{r}_1 \to \mathbf{y}_0$ *is output strictly passive. Furthermore, the gain of the system* Σ *is no larger than the value* $\frac{1}{\rho + \nu_0}$. □

3.2 Passivation Using Transfer Functions

For the purpose of passivation only, it is sufficient to use constant passivation parameters as in Section 3.1. However, it is often necessary that the system after passivation has other desired properties, for instance, being a low pass filter. In the following, we consider the passivation method using transfer functions as shown in Fig. 4. Through simple algebraic calculations, we can obtain the transfer function for system $u_0 \to y_0$ in Fig. 4, which is given by

$$\Pi_0 = \left(\frac{m_p + m_s G}{1 + m_f G}\right)\left(\frac{as + 1}{bs + 1}\right), \tag{12}$$

where the left bracket represents the system (4) and the right bracket represents the low pass filter H. It is obvious that by adding the low pass filter H in the parallel and series blocks, it is the same as cascading system (4) (i.e. $u_0 \to y_0$ in Fig. 3) with H. It is possible to use transfer functions in the feedback block, however, for simplicity, we assume that m_f is a constant in the present report.

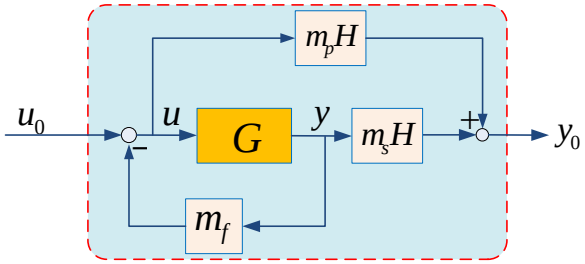

Figure 4: Passivation through series, parallel and feedback interconnection, where $m_p, m_f, m_s \in \mathbb{R}$. System H is given by a low-pass filter where $H = \frac{as+1}{bs+1}$ and $0 < a < b$.

Theorem 6. *Consider the the controller $G = Ke^{-\tau s}$ where $K > 0$ as shown in Fig. 4. Assume that $K|m_f| < 1$ and (8) is satisfied. If*

$$\frac{1}{a} - \frac{1}{b} \leq \frac{m_p + m_s m_f K^2 - |m_p m_f + m_s| K}{|m_s - m_f m_p| K\tau}. \tag{13}$$

then system $u_0 \to y_0$ is passive.

Proof. The frequency response for Π_0 is given by $\Pi_0(jw) = \bar{A} + j\bar{B}$, where

$$\bar{A} = \frac{\tilde{A}(abw^2+1) - (a-b)\tilde{B}w}{1+b^2w^2}, \quad \bar{B} = \frac{\tilde{A}(a-b)w + \tilde{B}(abw^2+1)}{1+b^2w^2},$$

where $\tilde{A}$ and $\tilde{B}$ are given by (10). The frequency-dependent IFP for Π_0 is given by

$$\nu_F(\Pi_0) = \frac{\tilde{A}(abw^2+1) - (a-b)\tilde{B}w}{1+b^2w^2}.$$

To guarantee $\nu_F(\Pi_0) \geq 0$ for all $w \in \mathbb{R}$, we need

$$h(w) \triangleq \tilde{A}(abw^2+1) - (a-b)\tilde{B}w \geq 0, \quad \forall w \in [0,\infty).$$

If (8) is satisfied, then we have $\tilde{A} \geq 0$. Further, if

$$\tilde{h}(w) = (m_p + m_s m_f K^2 - |m_p m_f + m_s| K)abw - (a-b)(m_s - m_f m_p)K\sin(\tau w) \geq 0,$$

for all $w \in [0,\infty)$, then $h(w) \geq w\tilde{h}(w) \geq 0$. Note that $\tilde{h}(0) = 0$, and its derivative

$$\dot{\tilde{h}}(w) \geq (m_p + m_s m_f K^2 - |m_p m_f + m_s| K)ab - (b-a)|m_s - m_f m_p|K\tau.$$

If in addition (13) is satisfied, then $\dot{\tilde{h}}(w) \geq 0$ and thus $\tilde{h}(w) \geq 0$ for all $w \in [0,\infty)$. Since $h(w) \geq w\tilde{h}(w) \geq 0$, we have $\nu_F(\Pi_0) \geq 0$ and thus system Π_0 is passive. □

Remark 7. *Theorem 6 provides sufficient conditions on the parameters (i.e. a and b) of the low pass filter H in order to guarantee passivity of the system Π_0. To apply the results, one can fix one parameter and find the feasible values for the other parameter. We note that the condition (13) may be conservative.*

3.3 PI controller with time delay

In Section 3.1 and Section 3.2, we assumed that the controller G is finite-gain stable, which does not include the case when the controller G is marginally stable, such as being a PI controller. In the following, we present the results for analyzing the IFP level for PI controllers with time delay.

Proposition 1. *Consider the pure time-delay transfer function $D(s) = e^{-\tau s}$. Then, $D(s)$ has delay-independent IFP $\nu = -1$.*

Proof. The frequency response for $D(s)$ is given by

$$D(jw) = \ e^{-\tau jw} = \ \cos(\tau w) - j\sin(\tau w).$$

Thus, the frequency-dependent IFP is given by

$$\nu_F(D) = \ \cos(\tau w) \geq \ -1,$$

for all $w \in \mathbb{R}$. Therefore, the IFP of $D(s)$,

$$\nu(D) = \ \min_{w\in\mathbb{R}} \nu_F(D) \geq \ -1. \tag{14}$$

On the other hand, when $w = \frac{\pi}{\tau}$, then

$$\nu_F(D, \frac{\pi}{\tau}) = \ -1.$$

Therefore, we have

$$\nu(D) \leq \ \nu_F(D, \frac{\pi}{\tau}) = \ -1. \tag{15}$$

From (14) and (15), we obtain that $\nu(D) = -1$. This completes the proof. □

Proposition 2. *Consider the transfer function $L(s) = \frac{1}{s}e^{-\tau s}$. Then, $L(s)$ has IFP $\nu = -\tau$.*

Proof. The frequency response for $L(s)$ is given by

$$L(jw) = \ \frac{1}{jw}(\cos(\tau w) - j\sin(\tau w)).$$

Thus, the frequency dependent IFP is given by

$$\nu_F(L) = \ -\frac{1}{w}\sin(\tau w).$$

When $w \to 0$, we have

$$\begin{aligned}\lim_{w\to 0} \frac{1}{w}\sin(\tau w) = \ & \tau \lim_{\tau w\to 0} \frac{1}{\tau w}\sin(\tau w) \\ = \ & \tau \lim_{\tau w\to 0} \cos(\tau w) = \ \tau.\end{aligned}$$

Thus, we have $\nu_F(L,0) = \ -\tau$ and the IFP of $L(s)$ satisfies

$$\nu(L) \leq \ \nu_F(L,0) = \ -\tau. \tag{16}$$

On the other hand, we have $f(w) \triangleq \ \nu_F(L) + \tau$ such that $f(0) = 0$ and

$$f(w) = \frac{1}{w}(\tau w - \sin(\tau w)).$$

Let us define $g(w) \triangleq \ \tau w - \sin(\tau w)$ so that $g(w) = 0$ and

$$\dot{g} = \ \tau(1 - \cos(\tau w)) \geq \ 0.$$

Thus, $g(w) \geq \ 0$ for all $w \geq \ 0$. Therefore, $f(w) \geq \ 0$ for all $w \geq \ 0$, i.e. $\nu_F(L) \geq \ -\tau$. Thus,

$$\nu(L) \geq \ -\tau. \tag{17}$$

Based on (16) and (17), we obtain that $\nu(L) = -\tau$. This completes the proof. □

Remark 8. *Consider the case when a transfer function can be written into sums of simple linear models, e.g.* $G = \ G_1 + G_2$, *where* G_1 *and* G_2 *are given by simple linear models. Due to the fact that*

$$\nu(G) \leq \ \nu(G_1) + \nu(G_2), \tag{18}$$

the IFP for system G *can be approximated by the IFP of simpler models* G_1 *and* G_2.

We consider when G is given by a PI controller cascaded with time-delay, i.e.

$$G(s) = (K_p + \frac{K_i}{s})e^{-\tau s}. \tag{19}$$

By applying the 'scaling property' of the IFP, we can simply calculate the IFP for $e^{-\tau s}$ and $\frac{1}{s}e^{-\tau s}$, which, respectively, are given by -1 and $-\tau$ according to Proposition 1-2. Thus, system $G(s)$ given by (19) has IFP that satisfies

$$\nu(G) \leq \ -K_p - K_i\tau,$$

such that $K_p + K_i\tau$ is a feedforward gain that can be used to passivate system $G(s)$. The following result is immediate.

Theorem 7. *Let the controller* G *be given by (19) and consider the passivation method in Fig. 3. The system* Σ_0 *given by (4) is passive if* $m_p \geq \ K_p + K_i\tau$, $m_f = \ 0$ *and* $m_s = \ 1$.

4 Optimization of Passivation Parameters

The passivation parameters m_p, m_f, m_s can be selected to optimize system performance in addition to guaranteeing passivity. If the mathematical relation between the performance and the parameters is known, then the performance evaluation can be done directly. If the relation is difficult to obtain or analyze, then the performance can be evaluated through simulation.

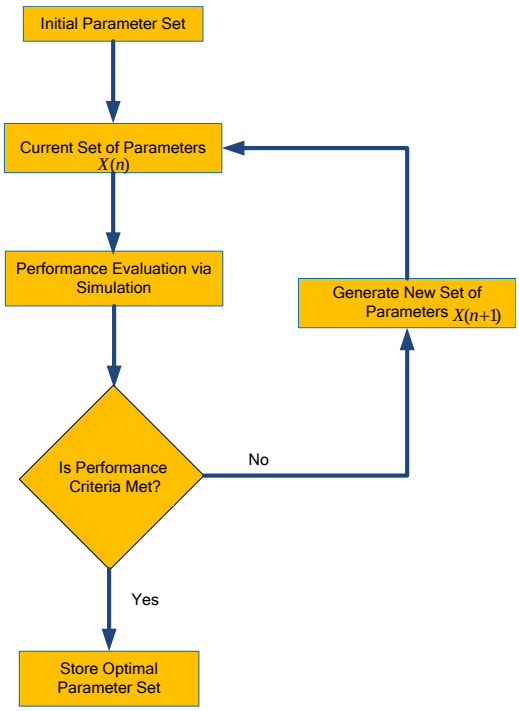

Figure 5: A functional diagram of the parameter learning method, where X denotes the set of parameters and n denotes the iteration number.

4.1 Parameter Learning for Performance Adaption

A functional diagram of the parameter learning system is shown in Fig. 5, where X denotes the set of parameters and n denotes the iteration number. Given particular values for the parameters, a performance index is evaluated via computer simulation. The learning method then determines the next set of parameters leading to an improved performance. The iterative procedure for performance evaluation and parameter updates is continued over many iterations until desired performance criteria are met. It is assumed that the system performance is measured via a performance index J, and the parameters in X and the performance index J are related by the following relation

$$J = f(X), \tag{20}$$

where the function $f(\cdot)$ is typically unknown. The performance of the system is actually evaluated using measurable quantities Y via a different equation

$$J = g(Y), \tag{21}$$

where the function $g(\cdot)$ is known. As the parameters of X vary, the measurements Y reflect the changes in the system performance, and J is evaluated via (21). To illustrate, X represents the passivation parameters, Y are measurable quantities such as output tracking error, while $g(\cdot)$ is chosen to be an integral of the norm of the tracking error over a finite time interval $[0, T]$.

Consider the feedback configuration in Fig. 6, where r_1 denotes the reference input, G denotes the controller and H denotes the physical plant. The passivation parameters are given by m_p, m_f

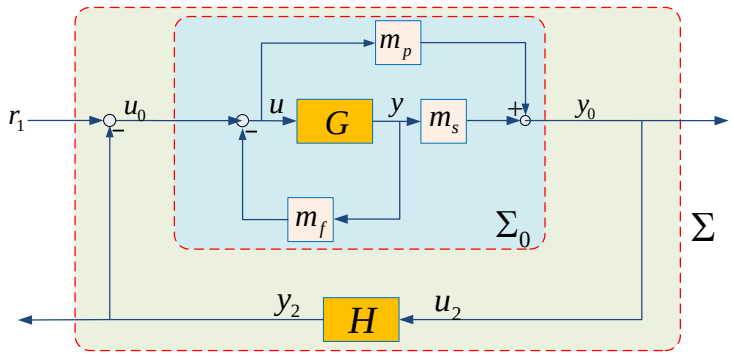

Figure 6: Feedback Interconnection of Two Systems with Passivation M.

and m_s. If the parameters are chosen to be $m_s = m_p = 1$, $m_f = 0$, then the dynamics for Σ_0 is the same with controller G. The optimization problem is summarized as follows,

$$\begin{array}{rl} \text{Minimize:} & J = \int_0^T \|r_1 - y_2\|^2 \mathrm{d}t \\ \text{w.r.t:} & m_p,\ m_s,\ m_f \\ \text{subject to:} & (4) \text{ being passive} \end{array} \tag{22}$$

where $r_1(t)$ is the reference input which may be time-varying, $T > 0$ denotes the time interval for one simulation cycle and the difference $r_1 - y_2$ represents the tracking error. It is important to note that if the dynamics for the plant are unknown (e.g. simulation models), or if the dynamics for the plant are complex (e.g. nonlinear or large-scale), then it is difficult to determine the analytic relation between performance and the parameters values.

4.2 Non-derivative Optimization Methods

A class of optimization algorithms, which only requires the availability of objective function values but no derivative information, is called derivative-free optimization algorithms. These numerical optimization methods can be used for system dynamics that are complex and cannot be presented with precise mathematical models. Problems in which derivatives are not available arise often in practice. For instance, the values of $f(X)$ can be the result of an experimental measurement or a stochastic simulation with underlying analytic form of f is unknown. One benefit of these optimization methods is that it does not require the gradient of the system model. Derivative-free optimization methods have been greatly studied. As the number and diversity of both faster computers and software designs developed for these methods increases, so does their applications in science and engineering [62, 63, 64, 65].

Given a deterministic objective function $f : R^n \to R$, the main assumption made is that this objective function does not have a well-defined set of derivatives hence the traditional methods for finding the minimum do not apply. Such situations arise if for instance is hard or expensive to evaluate or the environment is too noisy for developing a precise model. The long history of derivative-free algorithms goes back to 1960s and is marked by works of mathematicians such as W. Spendley, J. A. Nelder and R. Mead [66, 67]. Some examples of recent works on this subject are [68, 69, 70, 71]. Some of derivative free optimization methods have been adapted to solve

simple types of constraints, such as bounds. However a more efficient and generalized treatment of constraint optimization problems is still an open problem and subject to further investigations.

In the present report, we evaluate the performance via simulations and use the method of Hooke and Jeeves [72, 73] to solve the optimization problem (22). The method of Hooke and Jeeves performs two types of search – exploratory search and pattern search. Roughly speaking, given a point z_1, an exploratory search along the coordinate directions produces a new point z_2. Then the pattern search along the direction $z_2 - z_1$ leads to a new point w. Another exploratory search starting from w generates a new point z_3 and the next pattern search is along the direction $z_3 - z_2$. The process is repeated until a desired performance criteria is met. For more details of implementing the method of Hooke and Jeeves, we refer interested readers to [72].

5 Experimental Results in CarSim and Simulink

5.1 Adaptive Cruise Control Design

The main ideas behind this design of adaptive cruise control were adopted from Vanderbilt University model-based design of adaptive cruise control, explained in more details in [21]. In our work the passivation method, and passivity control are applied to the development of an adaptive cruise control, and we present experimental results that demonstrate the efficacy of our approach.

The vehicle equipped with the cruise control is a CarSim model of a C-Class Sedan, which weighs 1650 kg. The physical layer of our design is assumed to follow a given vehicle dynamic model. The longitudinal vehicle model is adopted from [9]. Two main assumptions are that the engine speed is algebraically proportional to the vehicle speed via gear ratios, and that the tire slip is negligible. The following equations with parameters summarized in Table 5.1 describe the longitudinal dynamics of our vehicle [21]:

$$\begin{aligned} T_e - R_g(T_b + M_r r + hF_a + mghsin\theta = &\ \beta a, \\ F_a = &\ C_a V^2, \\ \beta = &\ \frac{[J_e + R_g^2(J_{\omega r} + J_{\omega f} + mh^2)]}{R_g h}. \end{aligned}$$

The main function of the Adaptive Cruise Control is to maintain the desired velocity set by the driver. It is assumed that ACC uses a radar system which is attached to the front of the vehicle in order to detect and receive inputs from other vehicles on the road. The ACC needs to adjust its speed based on the desired speed of the vehicle, the speed of the lead vehicle, and the distance between the two cars. This means that our system will have a hybrid structure of two modes, one to control vehicle when it is accelerating, and one for when it is decelerating. The CarSim design structure is depicted in Figure 7. In upper level controller, the throttle control based on desired

Parameter	Definition
β	Lumped inertia
T_e	Net engine torque
T_b	Brake Torque
R_g	Gear Ratio
M_{rr}	Rolling resistance moments
h	Effective wheel radius
m	Total curb mass of the vehicle
J_e	Inertia of engine
$J_{\omega r}$	Inertia of rear axle
$J_{\omega f}$	Inertia of front axle
C_a	Aerodynamic drag coefficient
v	Velocity of the vehicle
a	Acceleration of the vehicle
F_a	Aerodynamic drag force
θ	Inclination angle of the road

Table 1: Vehicle Model Parameters

acceleration is defined as follows [21]:

$$\begin{aligned} a_1 &= k_1(v_d - v_h), \\ a_2 &= k_2(v_l - v) + k_3(S_d - S_a), \\ S_d &= \Delta + (v_h t_{gap}), \\ a_{des} &= \min(a_2, a_1). \end{aligned}$$

where k_1, k_2 and k_3 are gains for the controller, and v, v_d, v_l, v_h are respectively the current, desired, lead, and host velocities. In the absence of a leading vehicle, the host vehicle maintains a driver set velocity, essentially behaving like the conventional cruise control system. When a vehicle is detected by the radar, the ACC system will control the distance between the host vehicle and the leading vehicle, is Δ the desired distance maintained and S_d is the desired maintained for the case where the lead car comes to a sudden stop, and t_{gap} is time gap. The brake control is the following [21]:

$$T_b = k_b(P_{mc} - P_{po})$$

where P_{mc} and P_{po} are respectively desired brake cylinder pressure, and push-out pressure required to engine brake. The switching rule for the design is the following, when the desired acceleration is greater than the residual acceleration, the throttle mode turns on for the host car, otherwise the brake mode turns on [21]:

$$\begin{aligned} \text{Throttle mode} &= 1, \quad \text{if} \quad a_{des} > a_{res}, \\ \text{Brake mode} &= 1, \quad \text{if} \quad a_{des} < a_{res}. \end{aligned} \tag{23}$$

The lower level controller takes the desired acceleration as an input, and decides whether a brake or acceleration should be applied. The switching logic given in (23) where desired and residual

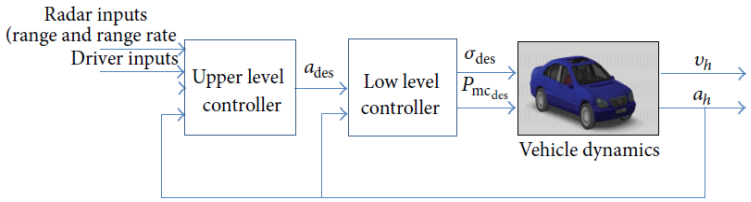

Figure 7: Adaptive Cruise Control Design Structure [21].

accelerations are compared, demonstrates this process. As a result of this decision, the desired throttle angel command or master cylinder pressure command is calculated and sent to the vehicle. An inverse engine map was used to turn the desired velocity into desired throttle angle required by CarSim as the input. Similarly, the desired brake torque is converted into an equivalent master cylinder pressure which is accepted by CarSim as the input.

5.2 A Co-simulation Framework

Increase in computational capability of computers, coupled with new mathematical programming techniques has produced a particulary promising methodology called co-simulation. The main purpose of this method is to address the control problem rising from the ever-increasing scale and complexity of large-scale systems [74]. Optimization plays a strong role in cosimulation, as most algorithms utilize an optimizer to minimize or maximize a cost function which is related to the system performance. Under cosimulation, the exact or approximated state-space model of the system is not required, and the control parameters are decide by input/output data coming from the system. In addition to this, the system is controlled under realistic conditions including physical constraints and uncommon and possible unpredictable behaviors. These two factors give co-simulation an advantage over other nonlinear control methods.

Under co-simulation control structure, a simulation model of the system is connected to a parameterized controller with parameters that are updated by an optimization algorithm. For each choice of parameter sets, the close loop system is simulated and a measure of the performance is provided to the optimizer [74]. The optimization side of co-simulation can be computationally heavy and cumbersome. Specifically for large scale systems, this process involves several states, great number of inputs, and parameters. Due to an absence of a well-defined state-space model for the system, the traditional gradient methods employing Jacobian and Hessian matrices are rendered useless for co-simulation algorithms. Consequently, derivative-free optimization methods play an important part in designing co-simulation controllers.

Figure 3 shows our design under co-simulation control structure. Hooke and Jeeves as an optimizer calculates and provides the parameter for the adaptive cruise control which controls the vehicle model. For each choice of parameters, the close loop system is simulated and a measure of performance is provided back to hooke and Jeeves program which accordingly decides whether the parameters should be updated in order to improve the performance.

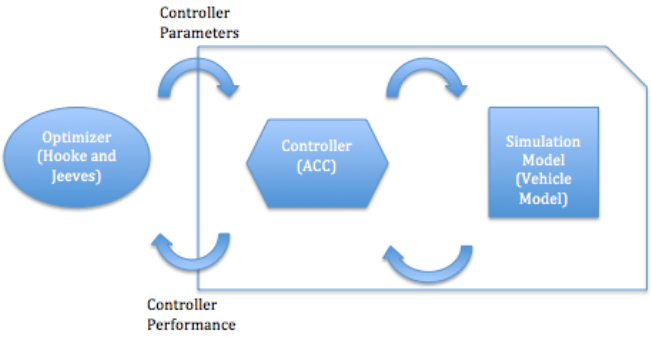

Figure 8: The design for Co-simulation and Adaptive Cruise Control.

5.3 Simulation Results

We present experimental results through CarSim and Simulink. CarSim is a software package that simulates the dynamic behavior of vehicles such as passenger cars, racecars, light trucks, and utility vehicles [75]. CarSim provides animations of simulated tests and outputs over hundreds of calculated variables, which can be plotted and analyzed in MATLAB. In our simulations, a vehicle dynamic model, created and configured in Carsim, was used to represent the plant and the controller was implemented in MATLAB/Simulink. A block diagram for our simulation setup is given in Fig. 6. The reference input r_1 is given by a time-varying trajectory that represents the desired velocity profile for the vehicle. The controller G is given by $G = Ke^{-\tau s}$. The input to the controller is the output tracking error $r_1 - y_2$. The plant model is given by CarSim whose dynamics is typically unknown. The output of the plant y_2 is the velocity of the vehicle. The control objective is to minimize output tracking error as we discussed in Section 4.

If the passivation parameters are set to be $m_p = m_f = 0$ and $m_s = 1$, then the dynamics for Σ_0 and the controller are the same. The initial values for the passivation parameters (in order to run the optimization algorithm) are selected such that the passivation condition (6) or (7) is satisfied. For every cycle $T = 25$ seconds, i.e. at the end of each cycle $t = T$, the cost function J is updated, and the new estimate of the parameter is computed for the next cycle according to the method of Hooke and Jeeves. The purpose of updating the passivation parameters is to improve the performance of the controller over many cycles, hence decreasing the tracking errors over time. In our simulations, we assume that the vehicle starts at velocity 65 km/h. To make the simulations more realistic, we assume that the delay in the controller is given by a uniformly distributed random number within the interval $[0.4, 0.6]$ seconds so that the expectation of the time delay is given by 0.5 seconds (we refer interested readers to [76] for more details).

5.3.1 When the Reference Input is a Constant

The desired velocity is set to be a constant, i.e. $r_1 = 80$ km/h. The passivation parameters obtained from the optimization algorithm are given by $m_f = 0$, $m_p = 2.9063$ and $m_s = 0.9063$. One can verify that the conditions derived in Theorem 4 are satisfied and the IFP level for Σ_0

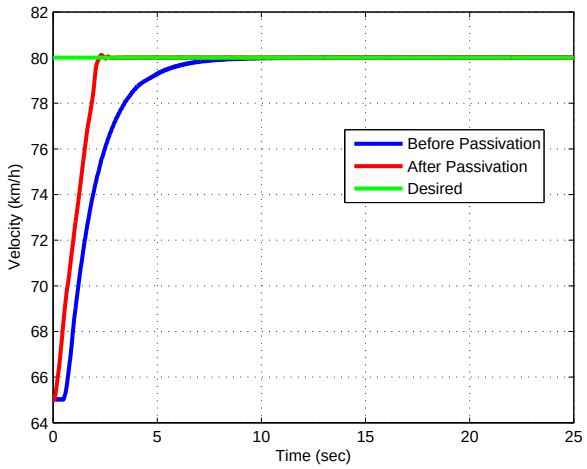

Figure 9: Velocity trajectories for constant input.

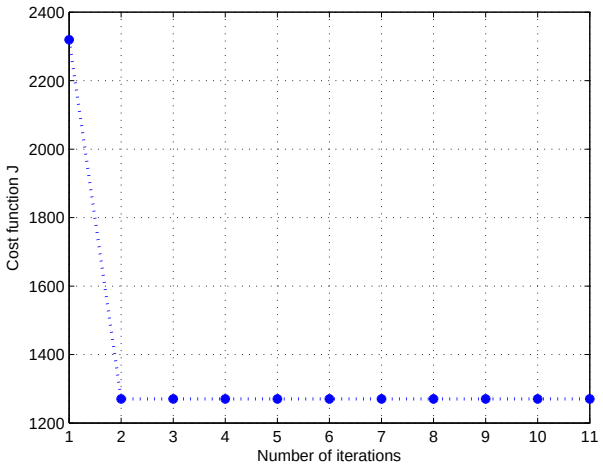

Figure 10: Cost function over iterations for constant input.

is given by 2.45. The simulation results are summarized in Fig. 9, 10, 11 and 12. As shown in Fig. 9, the desired velocity is achieved in 2.5 seconds after passivation, while it takes 8 seconds before passivation. As shown in Fig. 10, the cost function is decreasing over the iterations; after 10 iterations, the cost function has been reduced to approximately 50%. The acceleration trajectories in Fig. 11 show that the vehicle is accelerating to reach the 80 km/h and then remains a constant speed. The Nyquist plot of Σ_0 is shown in Fig. 12, where the IFP index of Σ_0 is approximately given by 2.45, which validates our results in Theorem 4.

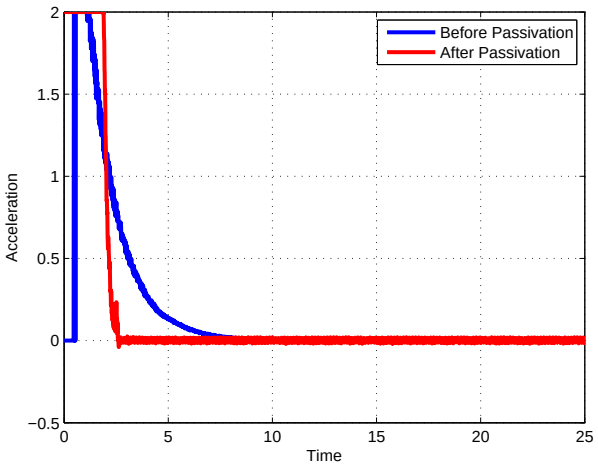

Figure 11: Acceleration trajectories for constant input.

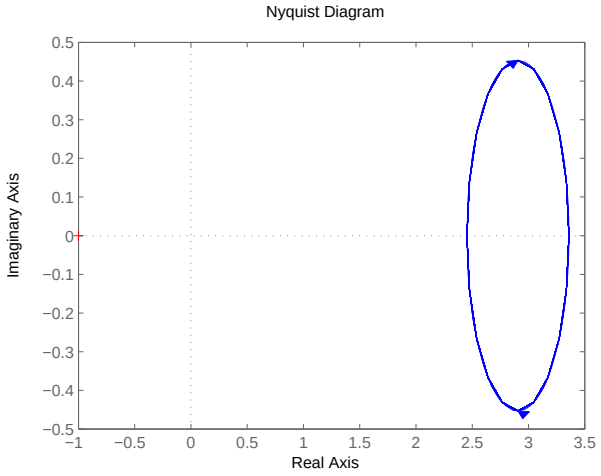

Figure 12: Nyquist plot of Σ_0 for constant input.

5.3.2 When the Reference Input is a Sinusoid Function

We consider the reference input is given by a sinusoid function $r_1 = 20\sin(0.1t)+60$. The passivation parameters obtained from the optimization algorithm are given by $m_f = 0$, $m_p = 33.0469$ and $m_s = 1.0469$. One can verify that the conditions derived in Theorem 4 are satisfied and the IFP level for Σ_0 is given by 32.5. The simulation results are summarized in Fig. 13, 14, 15 and 16. As shown in Fig. 13, the desired velocity is achieved in 1 seconds after passivation and our passivation method can greatly improve the tracking performance. As shown in Fig. 14, the cost function is decreasing over the iterations; after 10 iterations, the cost function has been reduced to approximately 5%. The acceleration trajectories in Fig. 15 show that the vehicle is speeding up or slowing down frequently in order to minimize the tracking error. The Nyquist plot of Σ_0 is shown

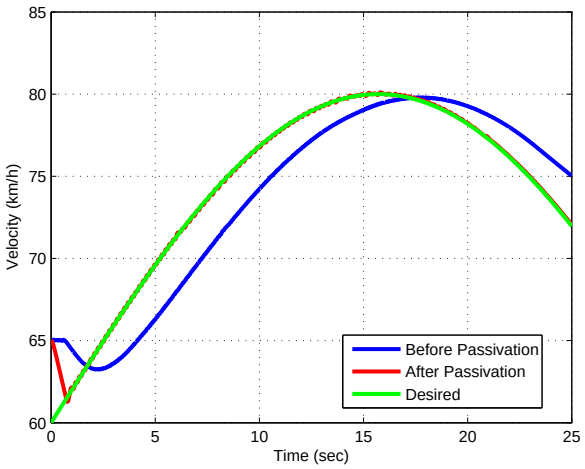

Figure 13: Velocity trajectories for sinusoid input.

in Fig. 16, where the IFP index of Σ_0 is approximately given by 32.5, which validates our results in Theorem 4. We point out that the "chattering" in the acceleration can be reduced if we use transfer functions as described in Section 3.2. As an example, we select the low pass filter H to be

$$H = \frac{0.08s + 1}{s + 1}. \tag{24}$$

The passivation parameters obtained from the following optimization algorithm are given by $m_f = 0.75$, $m_p = 25.125$ and $m_s = -17.75$, where

$$\begin{array}{rl} \text{Minimize:} & J = \int_0^T \|r_1 - y_2\|^2 \mathrm{d}t \\ \text{w.r.t:} & m_p,\ m_s,\ m_f \\ \text{subject to:} & (12) \text{ being passive} \end{array} \tag{25}$$

The simulation results are summarized in Fig. 17, 18, 19 and 20. Similar to the case using constant passivation parameters, it is shown in Fig. 17 and 18 that our passivation method using transfer functions can also greatly improve the tracking performance. Moreover, by adding the low pass filter, the acceleration trajectory can be smooth as shown in Fig. 19, which can be seen through animations in CarSim. Fig. 20 shows that the choice of (24) yields a passive controller Π_0.

5.3.3 When the Reference Input is a User-Specified Trajectory

We consider the reference input is a user-specified trajectory (which may be the velocity trajectory of the leading vehicle), where $r_1(t)$ is given by

$$r_1(t) = \begin{cases} 60, & \text{if } \ t \le \frac{1}{3}T \\ 60 + \frac{120}{T}(t - \frac{1}{3}T), & \text{if } \ \frac{1}{3}T \le t \le \frac{1}{2}T \\ 80, & \text{if } \ \frac{1}{2}T \le t \le \frac{2}{3}T \\ 55 + \frac{150}{T}(t - \frac{5}{6}T), & \text{if } \ \frac{2}{3}T \le t \le \frac{5}{6}T \\ 55, & \text{if } \ \frac{5}{6}T \le t \le T \end{cases}$$

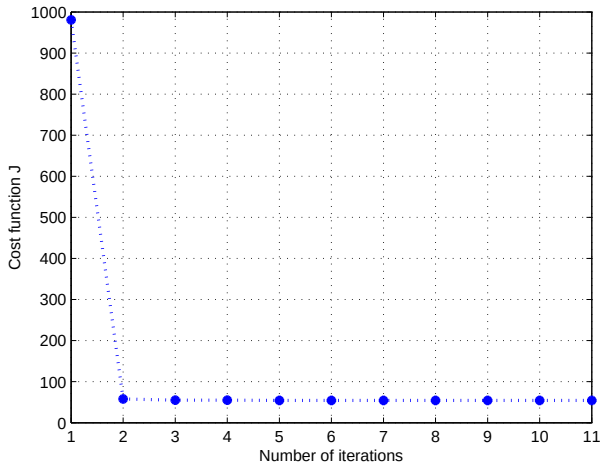

Figure 14: Cost function over iterations for sinusoid input.

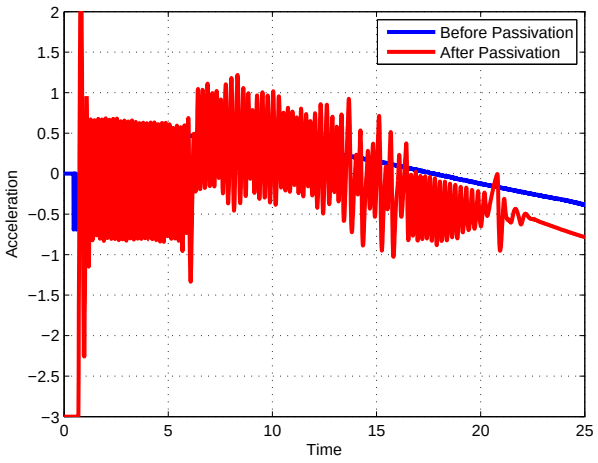

Figure 15: Acceleration trajectories for sinusoid input.

The passivation parameters obtained from the optimization algorithm are given by $m_f = 0$, $m_p = 23.25$ and $m_s = 8.5$. One can verify that the conditions derived in Theorem 4 are satisfied and the IFP level for Σ_0 is given by 19. The simulation results are summarized in Fig. 21, 22, 23 and 24. As shown in Fig. 21, our passivation method can greatly improve the tracking performance. As shown in Fig. 22, the cost function is decreasing over the iterations; after 10 iterations, the cost function has been reduced to approximately 4%. The acceleration trajectories in Fig. 23 show that the vehicle is speeding up or slowing down frequently within time intervals $[2, 8]$, $[13, 17]$ and $[22, 25]$ in order to minimize the tracking error. The Nyquist plot of Σ_0 is shown in Fig. 24, where the IFP index of Σ_0 is approximately given by 19, which validates our results in Theorem 4. Similar to the previous case, the "chattering" in the acceleration can be reduced if we use the low pass filter H given by (24). The passivation parameters obtained by solving the optimization problem

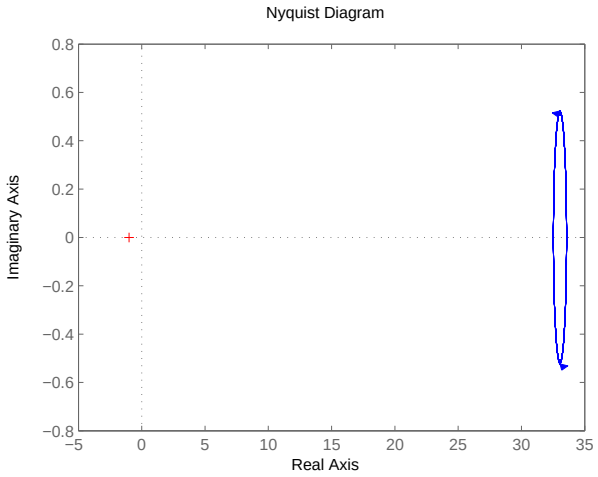

Figure 16: Nyquist plot of Σ_0 for sinusoid input.

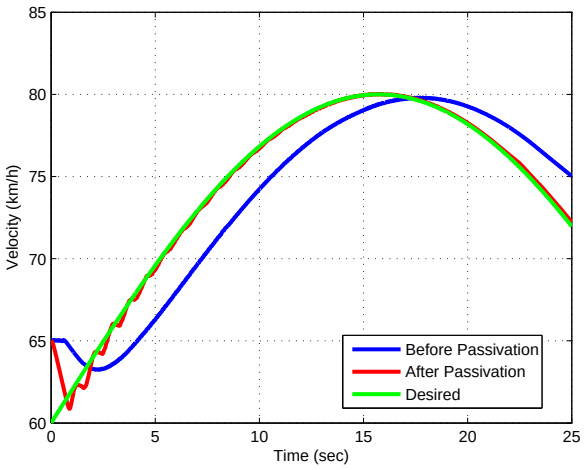

Figure 17: Velocity trajectories with low pass filter (24) for sinusoid input.

(25) are given by $m_f = 0.375$, $m_p = 24.755$ and $m_s = -27.125$. Similar to the case using constant passivation parameters, it is shown in Fig. 25 and 26 that our passivation method using transfer functions can also greatly improve the tracking performance. Moreover, by adding the low pass filter, the acceleration trajectory can be smooth as shown in Fig. 27, which can be seen through animations in CarSim. Fig. 28 shows that the choice of (24) yields a passive controller Π_0.

5.4 Discussion and Observations

We point out that the delays considered in our simulations are time-varying and the controller gain is fixed to be 0.5. From the simulation results in Section 5.3.1-5.3.3, we can make the following

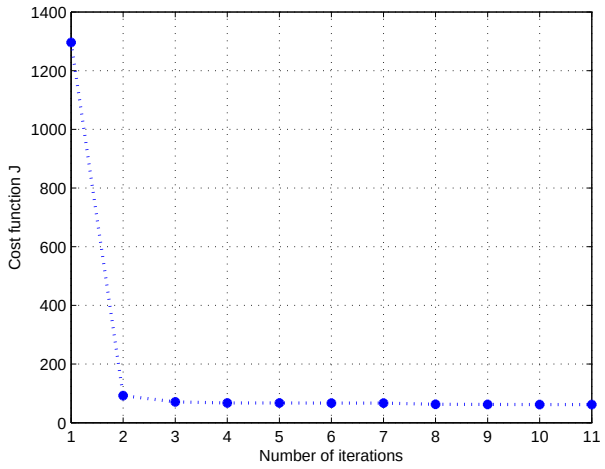

Figure 18: Cost function over iterations with low pass filter (24) for sinusoid input.

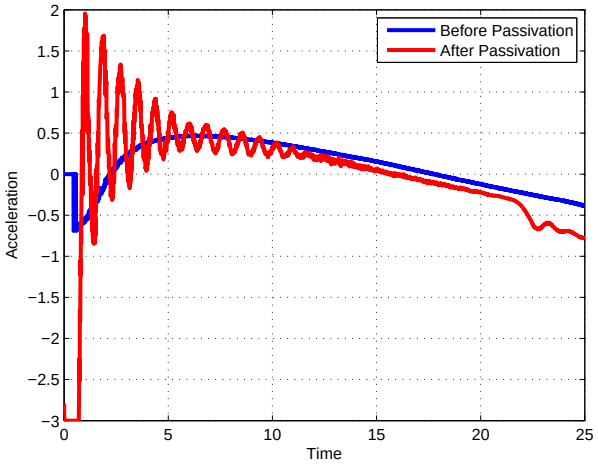

Figure 19: Acceleration trajectories with low pass filter (24) for sinusoid input.

observations. First, our passivation method can greatly improve the system performance in the presence of time delay beyond guaranteeing passivity. Second, our passivation method using transfer functions can take into account multiple performance criteria, such as minimizing the tracking error and smoothing the acceleration. Third, the method of Hooke and Jeeves which is a non-derivative optimization method can provide a local optimum in a few iterations. Finally, a controller with a large IFP level often provides good tracking performance, however, it may result in chattering in the acceleration. This implies that whether an optimal controller has a large IFP level is dependent on the performance criteria under consideration. The analytic relation between system performance and the IFP level needs to be further studied.

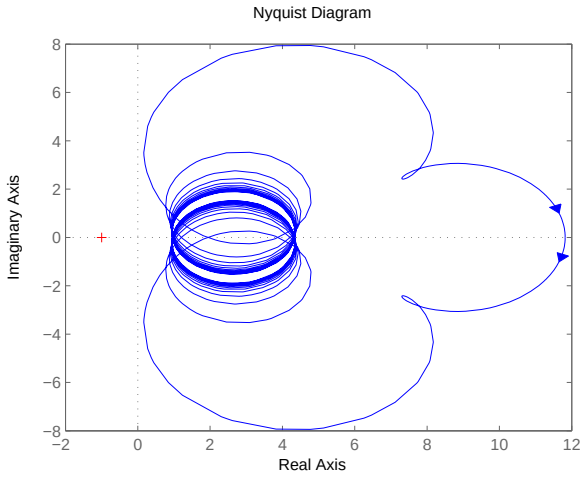

Figure 20: Nyquist plot of Π_0 for sinusoid input.

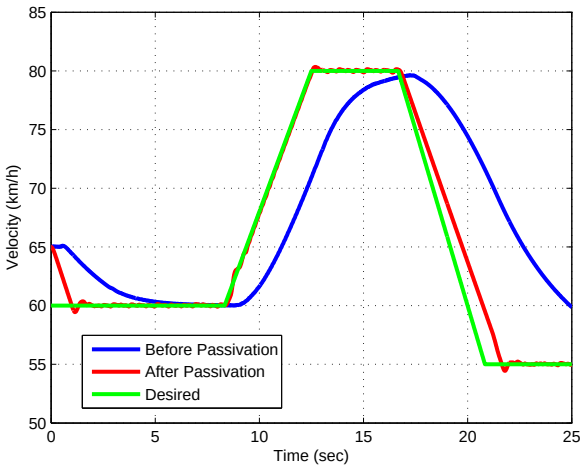

Figure 21: Velocity trajectories for a user-specified input.

6 Conclusion and Future Works

In this report, we consider a passivation method that uses an input-output transformation matrix. This matrix generalizes the commonly used methods of series, feedback and parallel (or feedforward) interconnections to passivate a system. Through an appropriate design of this matrix, positive passivity levels can be guaranteed for the system. The passivation parameters can be selected by solving an optimization problem such as minimizing the tracking error. As an application of our passivation method, we consider systems with input-output time delay. We show that our passivation method can be used to compensate for the time-delay in the controller and improve the closed-loop system performance. To validate our results, we provide simulation results in CarSim and Simulink. Future work may include: (1) considering both velocity control and spacing control

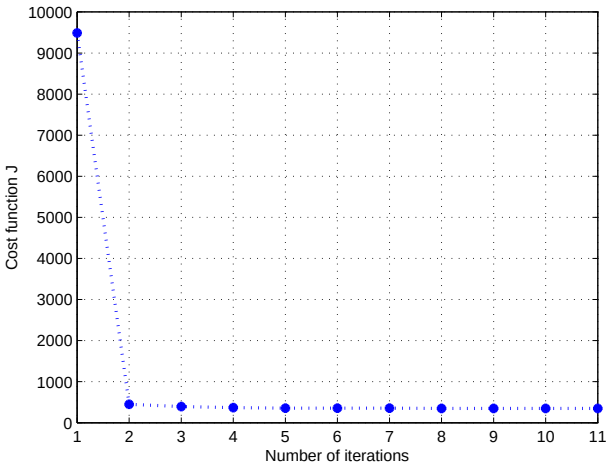

Figure 22: Cost function over iterations for a user-specified input.

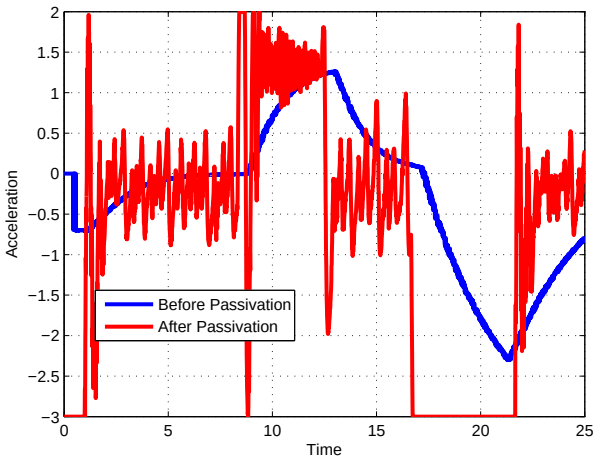

Figure 23: Acceleration trajectories for a user-specified input.

for adaptive cruise control of automotive systems; (2) investigating the interaction between adaptive cruise control and lane keeping control or other control algorithms for automobiles; (3) establishing analytic relations between system performance and the passivation parameters; (4) considering general linear or nonlinear operators for passivation.

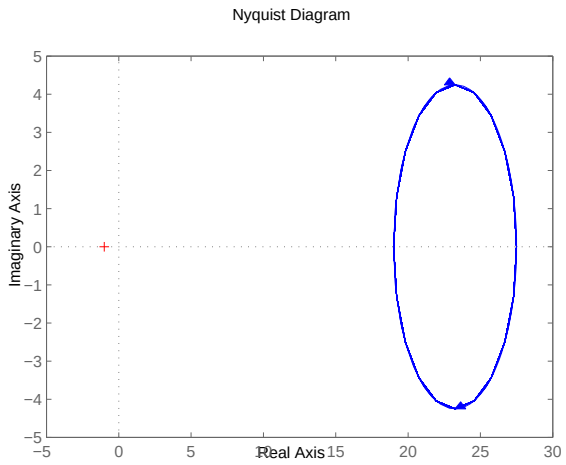

Figure 24: Nyquist plot of Σ_0 for a user-specified input.

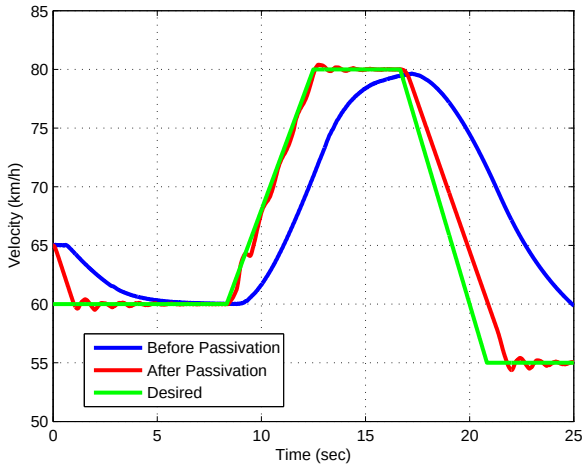

Figure 25: Velocity trajectories with low pass filter (24) for a user-specified input.

7 Appendix: Proof of Theorem 3

Proof. For notational convenience, we denote $\langle u, y\rangle_T = \int_0^T u^T y \, \mathrm{d}t$. Since $u_0 = u + m_f y$ and $y_0 = m_p u + m_s y$, it can be easily shown that

$$\begin{aligned} \langle u_0, y_0\rangle_T &= m_p\langle u, u\rangle_T + m_f m_s\langle y, y\rangle_T \\ &\quad + (m_s + m_f m_p)\langle u, y\rangle_T, \end{aligned} \tag{26}$$

$$\langle u_0, u_0\rangle_T = \langle u, u\rangle_T + 2m_f\langle u, y\rangle_T + m_f^2\langle y, y\rangle_T, \tag{27}$$

$$\langle y_0, y_0\rangle_T = m_p^2\langle u, u\rangle_T + 2m_p m_s\langle u, y\rangle_T + m_s^2\langle y, y\rangle_T. \tag{28}$$

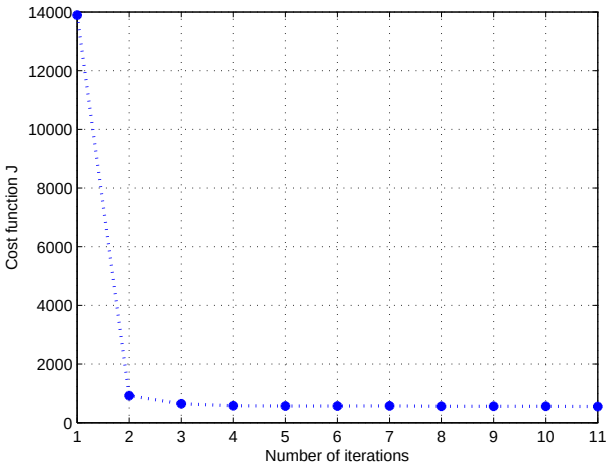

Figure 26: Cost function over iterations with low pass filter (24) for a user-specified input.

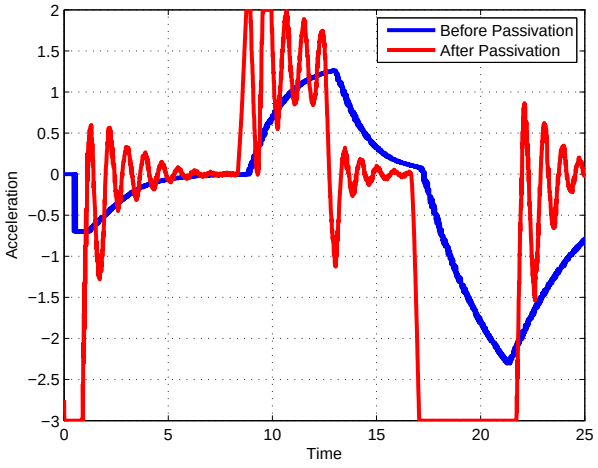

Figure 27: Acceleration trajectories with low pass filter (24) for a user-specified input.

Since system G is finite gain stable with gain γ, we have

$$\langle y, y\rangle_T \leq \gamma^2 \langle u, u\rangle_T. \tag{29}$$

(i). To find an OFP level of the system $\mathbf{u}_0 \to \mathbf{y}_0$, we use (26), (28) and the following relation

$$\begin{aligned} &\langle u_0, y_0\rangle_T - \rho_0 \langle y_0, y_0\rangle_T \\ &= (m_p - \rho_0 m_p^2)\langle u, u\rangle_T + (m_f m_s - \rho_0 m_s^2)\langle y, y\rangle_T \\ &\quad + (m_s + m_f m_p - 2\rho_0 m_p m_s)\langle u, y\rangle_T. \end{aligned}$$

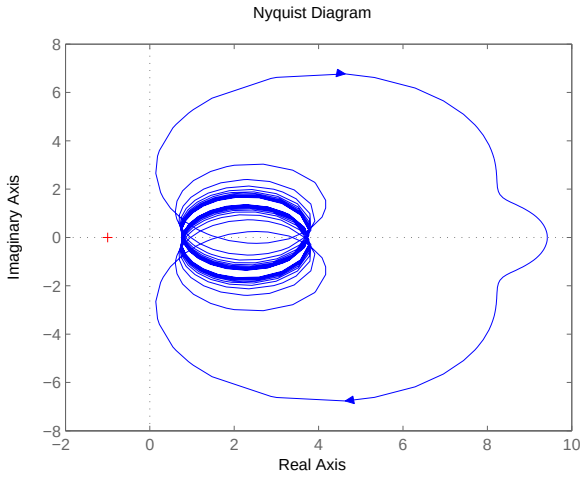

Figure 28: Nyquist plot of Σ_0 with low pass filter (24) for a user-specified input.

Since $2\rho_0 m_p m_s = m_s + m_f m_p$, we have

$$\begin{aligned}&\langle u_0, y_0\rangle_T - \rho_0\langle y_0, y_0\rangle_T\\ =\ &(m_p - \rho_0 m_p^2)\langle u, u\rangle_T + (m_f m_s - \rho_0 m_s^2)\langle y, y\rangle_T.\end{aligned}$$

If m_p, m_s, m_f are chosen such that (6) holds, then we have

$$\begin{aligned}m_f m_s - \rho_0 m_s^2 &= m_s^2\left(\frac{m_f}{m_s} - \rho_0\right)\\ &= \frac{1}{2}m_s^2\left(\frac{m_f}{m_s} - \frac{1}{m_p}\right)\\ &= \frac{1}{2}\frac{m_s}{m_p}\left(m_f m_p - m_s\right)\\ &< 0.\end{aligned}$$

Further, we can derive that $\frac{m_f}{m_s} - \rho_0 < 0$, then based on the fact that $\frac{1}{m_p} - \rho_0 = \rho_0 - \frac{m_f}{m_s}$, we have $\frac{1}{m_p} - \rho_0 > 0$. Then, from (29), we can obtain that

$$\begin{aligned}&\langle u_0, y_0\rangle_T - \rho_0\langle y_0, y_0\rangle_T\\ \geq\ &(m_p - \rho_0 m_p^2)\langle u, u\rangle_T - \gamma^2(\rho_0 m_s^2 - m_f m_s)\langle u, u\rangle_T\\ =\ &\left[m_p^2(\frac{1}{m_p} - \rho_0) - m_s^2\gamma^2(\rho_0 - \frac{m_f}{m_s})\right]\langle u, u\rangle_T\\ =\ &(\frac{1}{m_p} - \rho_0)\left(m_p^2 - m_s^2\gamma^2\right)\langle u, u\rangle_T.\end{aligned}$$

Then, from the condition $m_p \geq m_s\gamma > 0$, we can obtain

$$\langle u_0, y_0\rangle_T - \rho_0\langle y_0, y_0\rangle_T \geq 0.$$

Therefore, the system $\mathbf{u}_0 \to \mathbf{y}_0$ has OFP($\rho_0 > 0$).

(ii). To find an IFP level of the system $\mathbf{u}_0 \to \mathbf{y}_0$, we use (26), (27) and the following relation

$$\begin{aligned}
&\langle u_0, y_0\rangle_T - \nu_0\langle u_0, u_0\rangle_T \\
&= (m_p - \nu_0)\langle u, u\rangle_T + (m_f m_s - \nu_0 m_f^2)\langle y, y\rangle_T \\
&\quad + (m_s + m_f m_p - 2\nu_0 m_f)\langle u, y\rangle_T
\end{aligned}$$

Since $2\nu_0 m_f = m_f m_p + m_s$, we have

$$\begin{aligned}
&\langle u_0, y_0\rangle_T - \nu_0\langle u_0, u_0\rangle_T \\
&= (m_p - \nu_0)\langle u, u\rangle_T + (m_f m_s - \nu_0 m_f^2)\langle y, y\rangle_T.
\end{aligned}$$

If m_p, m_s, m_f are chosen such that (7) holds, then we have

$$\begin{aligned}
m_f m_s - \nu_0 m_f^2 &= m_f^2\left(\frac{m_s}{m_f} - \nu_0\right) \\
&= \frac{1}{2}m_f^2\left(\frac{m_s}{m_f} - m_p\right) \\
&= \frac{1}{2}m_f\left(m_s - m_f m_p\right) \\
&< 0.
\end{aligned}$$

Further, we can derive that $\frac{m_s}{m_f} - \nu_0 < 0$, then based on the fact that $m_p - \nu_0 = \nu_0 - \frac{m_s}{m_f}$, we have $m_p - \nu_0 > 0$. Then, from (29), we can obtain that

$$\begin{aligned}
&\langle u_0, y_0\rangle_T - \nu_0\langle u_0, u_0\rangle_T \\
&\geq (m_p - \nu_0)\langle u, u\rangle_T + (m_f m_s - \nu_0 m_f^2)\gamma^2\langle u, u\rangle_T \\
&= \left[(m_p - \nu_0) - m_f^2\gamma^2(\nu_0 - \frac{m_s}{m_f})\right]\langle u, u\rangle_T \\
&= (m_p - \nu_0)\left(1 - m_f^2\gamma^2\right)\langle u, u\rangle_T.
\end{aligned}$$

Then, from the condition $m_{11} \geq m_{12}\gamma > 0$, we can obtain

$$\langle u_0, y_0\rangle_T - \nu_0\langle u_0, u_0\rangle_T \geq 0.$$

Therefore, the system $\mathbf{u}_0 \to \mathbf{y}_0$ has IFP($\nu_0 > 0$). □

References

[1] P. J. Antsaklis, M. J. McCourt, H. Yu, P. Wu, and F. Zhu, "Cyber-physical systems design using dissipativity," in *Control Conference (CCC), 2012 31st Chinese.* IEEE, 2012, pp. 1–5.

[2] D. Shang, E. Eyisi, Z. Zhang, X. Koutsoukos, J. Porter, G. Karsai, and J. Sztipanovits, "A case study on the model-based design and integration of automotive cyber-physical systems," in *Control & Automation (MED), 2013 21st Mediterranean Conference on.* IEEE, 2013, pp. 483–492.

[3] J. Bao and P. L. Lee, *Process control: the passive systems approach.* Springer Science & Business Media, 2007.

[4] D. Hill and P. Moylan, "The stability of nonlinear dissipative systems," *Automatic Control, IEEE Transactions on*, vol. 21, no. 5, pp. 708 – 711, Oct. 1976.

[5] R. Ortega, A. J. Van Der Schaft, I. Mareels, and B. Maschke, "Putting energy back in control," *Control Systems, IEEE*, vol. 21, no. 2, pp. 18–33, 2001.

[6] M. Zefran, F. Bullo, and M. Stein, "A notion of passivity for hybrid systems," in *Decision and Control, 2001. Proceedings of the 40th IEEE Conference on*, vol. 1. IEEE, 2001, pp. 768–773.

[7] J. Zhao and D. J. Hill, "Dissipativity theory for switched systems," *Automatic Control, IEEE Transactions on*, vol. 53, no. 4, pp. 941–953, 2008.

[8] J. Gerdes and J. Hedrick, "Vehicle speed and spacing control via coordinated throttle and brake actuation," *Control Engineering Practice*, vol. 5, no. 11, pp. 1607–1614, 1997.

[9] J. Hedrick and P. Yip, "Multiple sliding surface control: theory and application," *Journal of dynamic systems, measurement, and control*, vol. 122, no. 4, pp. 586–593, 2000.

[10] P. A. Ioannou and C.-C. Chien, "Autonomous intelligent cruise control," *Vehicular Technology, IEEE Transactions on*, vol. 42, no. 4, pp. 657–672, 1993.

[11] K. Yi, S. Lee, and Y. Kwon, "An investigation of intelligent cruise control laws for passenger vehicles," *Proceedings of the Institution of Mechanical Engineers, Part D: Journal of Automobile Engineering*, vol. 215, no. 2, pp. 159–169, 2001.

[12] P. Fancher, H. Peng, and Z. Bareket, "Comparative analyses of three types of headway control systems for heavy commercial vehicles," *Vehicle System Dynamics*, vol. 25, no. S1, pp. 139–151, 1996.

[13] B. A. Guvenc and E. Kural, "Adaptive cruise control simulator: a low-cost, multiple-driver-in-the-loop simulator," *Control Systems, IEEE*, vol. 26, no. 3, pp. 42–55, 2006.

[14] K. Breuer and M. Weilkes, "A versatile test-vehicle for acc-systems and components," in *Euromotor-Seminar Telematic/Vehicle and Environment-" Adaptive Cruise Control, Series Introduction and Future Development*, 1999.

[15] A. R. Girard, S. Spry, and J. K. Hedrick, "Intelligent cruise control applications: Real-time embedded hybrid control software," *Robotics & Automation Magazine, IEEE*, vol. 12, no. 1, pp. 22–28, 2005.

[16] H. Raza and P. Ioannou, "Vehicle following control design for automated highway systems," *Control Systems, IEEE*, vol. 16, no. 6, pp. 43–60, 1996.

[17] X.-Y. Lu, H.-S. Tan, S. Shladover, and J. K. Hedrick, "Nonlinear longitudinal controller implementation and comparison for automated cars," *Journal of Dynamic Systems, Measurement, and Control*, vol. 123, no. 2, pp. 161–167, 2001.

[18] S. Dermann and R. Isermann, "Nonlinear distance and cruise control for passenger cars," in *American Control Conference, Proceedings of the 1995*, vol. 5. IEEE, 1995, pp. 3081–3085.

[19] H. Holzmann, C. Halfmann, S. Germann, M. Würtenberger, and R. Isermann, "Longitudinal and lateral control and supervision of autonomous intelligent vehicles," *Control Engineering Practice*, vol. 5, no. 11, pp. 1599–1605, 1997.

[20] A. Stefanopoulou and L. Moklegaard, "Adaptive continuously variable compression braking control for heavy-duty vehicles," *Ann Arbor*, vol. 1001, p. 48197, 2002.

[21] E. Eyisi, Z. Zhang, X. Koutsoukos, J. Porter, G. Karsai, and J. Sztipanovits, "Model-based control design and integration of cyberphysical systems: an adaptive cruise control case study," *Journal of Control Science and Engineering*, vol. 2013, p. 1, 2013.

[22] Q.-G. Wang, T. H. Lee, and K. K. Tan, *Finite-spectrum assignment for time-delay systems*. Springer Science & Business Media, 1998, vol. 239.

[23] O. J. Smith, "A controller to overcome dead time," *ISA Journal*, vol. 6, no. 2, pp. 28–33, 1959.

[24] J. Jang *et al.*, "Adaptive control design with guaranteed margins for nonlinear plants," Ph.D. dissertation, Massachusetts Institute of Technology, 2009.

[25] S.-I. Niculescu and A. M. Annaswamy, "An adaptive smith-controller for time-delay systems with relative degree n 2," *Systems & control letters*, vol. 49, no. 5, pp. 347–358, 2003.

[26] D. Kim and J. Park, "Application of adaptive control to the fluctuation of engine speed at idle," *Information Sciences*, vol. 177, no. 16, pp. 3341–3355, 2007.

[27] R. Ortega and R. Lozano, "Globally stable adaptive controller for systems with delay," *International Journal of Control*, vol. 47, no. 1, pp. 17–23, 1988.

[28] V. Kolmanovskii and A. Myshkis, *Introduction to the theory and applications of functional differential equations*. Springer Science & Business Media, 1999, vol. 463.

[29] S.-I. Niculescu, *Delay effects on stability: a robust control approach*. Springer Science & Business Media, 2001, vol. 269.

[30] J.-P. Richard, "Time-delay systems: an overview of some recent advances and open problems," *automatica*, vol. 39, no. 10, pp. 1667–1694, 2003.

[31] K. Gu and S.-I. Niculescu, "Survey on recent results in the stability and control of time-delay systems*," *Journal of Dynamic Systems, Measurement, and Control*, vol. 125, no. 2, pp. 158–165, 2003.

[32] T. Legouis, A. Laneville, P. Bourassa, and G. Payre, "Characterization of dynamic vehicle stability using two models of the human pilot behaviour," *Vehicle System Dynamics*, vol. 15, no. 1, pp. 1–18, 1986.

[33] K. Guo and H. Guan, "Modelling of driver/vehicle directional control system," *Vehicle System Dynamics*, vol. 22, no. 3-4, pp. 141–184, 1993.

[34] D. T. McRuer and E. S. Krendel, "Mathematical models of human pilot behavior," DTIC Document, Tech. Rep., 1974.

[35] Z. Liu, G. Payre, and P. Bourassa, "Nonlinear oscillations and chaotic motions in a road vehicle system with driver steering control," *Nonlinear Dynamics*, vol. 9, no. 3, pp. 281–304, 1996.

[36] G. Orosz and G. Stépán, "Subcritical hopf bifurcations in a car-following model with reaction-time delay," *Proceedings of the Royal Society A: Mathematical, Physical and Engineering Science*, vol. 462, no. 2073, pp. 2643–2670, 2006.

[37] L. Davis, "Stability of adaptive cruise control systems taking account of vehicle response time and delay," *Physics Letters A*, vol. 376, no. 40, pp. 2658–2662, 2012.

[38] M. Bando, K. Hasebe, K. Nakanishi, and A. Nakayama, "Analysis of optimal velocity model with explicit delay," *Physical Review E*, vol. 58, no. 5, p. 5429, 1998.

[39] T. Nagatani and K. Nakanishi, "Delay effect on phase transitions in traffic dynamics," *Physical Review E*, vol. 57, no. 6, p. 6415, 1998.

[40] G. Orosz, J. Moehlis, and F. Bullo, "Robotic reactions: Delay-induced patterns in autonomous vehicle systems," *Physical Review E*, vol. 81, no. 2, p. 025204, 2010.

[41] ——, "Delayed car-following dynamics for human and robotic drivers," in *ASME 2011 International Design Engineering Technical Conferences and Computers and Information in Engineering Conference*. American Society of Mechanical Engineers, 2011, pp. 529–538.

[42] C. Scherer, P. Gahinet, and M. Chilali, "Multiobjective output-feedback control via lmi optimization," *Automatic Control, IEEE Transactions on*, vol. 42, no. 7, pp. 896–911, Jul 1997.

[43] M. Xia, P. Antsaklis, and V. Gupta, "Passivity analysis of a system and its approximation," in *American Control Conference (ACC), 2013*, June 2013, pp. 296–301.

[44] R. Lozano, B. Brogliato, O.Egeland, and B. Maschke, *Dissipative Systems Analysis and Control: Theory and Applications*, 1st ed. London: Springer, 2000.

[45] J. R. Forbes and C. J. Damaren, "Design of optimal strictly positive real controllers using numerical optimization for the control of flexible robotic systems," *Journal of the Franklin Institute*, vol. 348, no. 8, pp. 2191 – 2215, 2011.

[46] A. van der Schaft, *L2-Gain and Passivity Techniques in Nonlinear Control*, 2nd ed. Springer, 2000.

[47] R. Sepulchre, M. Jankovic, and P. Kokotovic, *Constructive Nonlinear Control*. Springer, 1994.

[48] H. Yu, F. Zhu, M. Xia, and P. J. Antsaklis, "Robust stabilizing output feedback nonlinear model predictive control by using passivity and dissipativity," in *European Control Conference (ECC), 2013*, Jul. 2013.

[49] J. C. Willems, "Dissipative dynamical systems part ii: Linear systems with quadratic supply rates," *Archive for Rational Mechanics and Analysis*, vol. 45, pp. 352–393, 1972.

[50] G. Fernndez-Anaya, J. lvarez Ramrez, and J.-J. Flores-Godoy, "Preservation of stability and passivity in irrational transfer functions," pp. 84–88, 2006.

[51] J. Bao and P. L. Lee, *Process Control: The passive systems approach*, 1st ed. Springer-Verlag, Advances in Industrial Control, London, 2007.

[52] J. T. Wen, "Robustness analysis based on passivity," in *American Control Conference, 1988*, 1988, pp. 1207–1213.

[53] H. K. Khalil, *Nonlinear Systems*, 3rd ed. Prentice Hall, Upper Saddle River, New Jersey, 2002.

[54] M. Xia, P. Antsaklis, and V. Gupta, "Passivity analysis of human as a controller," pp. 1–24, Aug. 2014. [Online]. Available: http://www3.nd.edu/ isis/techreports/isis-2014-002.pdf

[55] S. Hirche and M. Buss, "Human-oriented control for haptic teleoperation," *Proceedings of the IEEE*, vol. 100, no. 3, pp. 623–647, 2012.

[56] A. Kelkar and S. Joshi, "Robust passification and control of non-passive systems," in *American Control Conference*, Jun. 1998, pp. 3133–3137.

[57] A. Kelkar, Y. Mao, and S. Joshi, "Lmi-based passification for control of non-passive systems," in *American Control Conference, 2000. Proceedings of the 2000.* IEEE, 2000, pp. 1271–1275.

[58] L. Xie, M. Fu, and H. Li, "Passivity analysis and passification for uncertain signal processing systems," *Signal Processing, IEEE Transactions on*, vol. 46, no. 9, pp. 2394–2403, 1998.

[59] M. Xia, P. J. Antsaklis, and V. Gupta, "Passivity indices and passivation of systems with application to systems with input/output delay," in *53rd IEEE Conference on Decision and Control (CDC)*, Dec. 2014, pp. 783–788.

[60] M. Xia, A. Rahnama, S. Wang, and P. J. Antsaklis, "On guaranteeing passivity and performance with a human controller," in *23rd Meditteranean Conference on Control and Automation (MED)*, 2015, submitted.

[61] N. Kottenstette, M. J. McCourt, M. Xia, V. Gupta, and P. J. Antsaklis, "On relationships among passivity, positive realness, and dissipativity in linear systems," *Automatica*, vol. 50, no. 4, pp. 1003 – 1016, 2014.

[62] S. N. Deming, L. R. Parker Jr, and M. Bonner Denton, "A review of simplex optimization in analytical chemistry," 1978.

[63] G. A. Gray, T. G. Kolda, K. Sale, and M. M. Young, "Optimizing an empirical scoring function for transmembrane protein structure determination," *INFORMS Journal on Computing*, vol. 16, no. 4, pp. 406–418, 2004.

[64] J. M. Gablonsky, "Modifications of the direct algorithm." 2001.

[65] M. A. Abramson, "Pattern search algorithms for mixed variable general constrained optimization problems," Ph.D. dissertation, Citeseer, 2002.

[66] W. Spendley, G. R. Hext, and F. R. Himsworth, "Sequential application of simplex designs in optimisation and evolutionary operation," *Technometrics*, vol. 4, no. 4, pp. 441–461, 1962.

[67] J. A. Nelder and R. Mead, "A simplex method for function minimization," *The computer journal*, vol. 7, no. 4, pp. 308–313, 1965.

[68] V. Torczon, "On the convergence of the multidirectional search algorithm," *SIAM journal on Optimization*, vol. 1, no. 1, pp. 123–145, 1991.

[69] A. R. Conn, K. Scheinberg, and P. L. Toint, "On the convergence of derivative-free methods for unconstrained optimization," *Approximation theory and optimization: tributes to MJD Powell*, pp. 83–108, 1997.

[70] A. J. Booker, J. Dennis Jr, P. D. Frank, D. B. Serafini, V. Torczon, and M. W. Trosset, "A rigorous framework for optimization of expensive functions by surrogates," *Structural optimization*, vol. 17, no. 1, pp. 1–13, 1999.

[71] A. R. Conn, K. Scheinberg, and L. N. Vicente, *Introduction to derivative-free optimization*. Siam, 2009, vol. 8.

[72] R. Hooke and T. A. Jeeves, "Direct search solution of numerical and statistical problems," *Journal of the ACM (JACM)*, vol. 8, no. 2, pp. 212–229, 1961.

[73] M. D. Peek and P. J. Antsaklis, "Parameter learning for performance adaptation," *Control Systems Magazine, IEEE*, vol. 10, no. 7, pp. 3–11, 1990.

[74] S. Baldi, I. Michailidis, E. Kosmatopoulos, and P. Ioannou, "A "plug and play" computationally efficient approach for control design of large-scale nonlinear systems using cosimulation: A combination of two ingredients," *Control Systems, IEEE*, vol. 34, no. 5, pp. 56–71, 2014.

[75] C. U. Manual, "Mechanical simulation corporation," *Ann Arbor, MI*, vol. 48013, 2002.

[76] R. Rajamani, *Vehicle dynamics and control*. Springer Science & Business Media, 2011.